ANALYSIS OF DELAMINATIONS AND BONDED JOINTS

H. Rapp, Institut für Leichtbau, Universität der Bundeswehr München, Germany
H. Bansemir, Eurocopter Deutschland GmbH, Germany

Summary

In structures made from fibre reinforced materials changes in the wall thickness of laminates can only be accomplished by adding or dropping additional layers to the existing laminate. Depending on the taper angle and their thicknesses these additional layers are more or less sensitive to delamination due to in-plane forces and moments. The taper angle together with the stiffness of the added layer is an important number for strength considerations. The structural analysis of this problem can be done by the shear-lag theory. This theory applies to the determination of the behaviour of bonded joints as well. Another way to analyse the strength behaviour of delaminations and bonded joints is to use energy approaches like the strain energy release rate known from fracture mechanics. This energy approach shows some advantages over the stress analysis because there have less strength parameters to be known. The similarities and differences of both approaches are shown and discussed. Examples of application and results from experiments show the applicability of the strain energy procedure.

1. INTRODUCTION

In lightweight structures, wall thicknesses of each component have to be tailored regarding to the local loading. This means that the wall thickness has to change from one location to another. For components made from fibre reinforced materials, those changes of laminate thicknesses can only be accomplished by adding or dropping individual layers to or from a continuous laminate (Fig. 1). A characteristic value for such a change in wall thickness is the taper angle α defined by the ratio of overlap length l_i to layer thickness t_i. The larger this taper angle, the higher is the sensitivity of the added or dropped layers to delaminate.

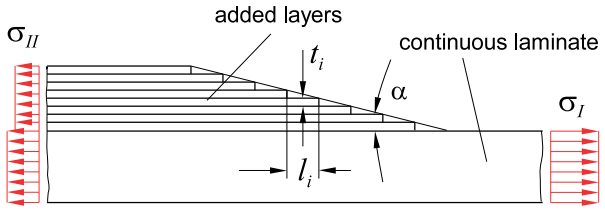

Fig. 1. Tapered laminate

Structural analysis of this task can be done in various ways. In [1] a review of common procedures for tapered laminates is given. These procedures can either be stress based by the use of the finite element method or by analytical methods, or they can be based on energy methods like the strain-energy release rate known from fracture mechanics.

The most simple stress analysis is done by the well analytical shear lag theory [2], [3]. More modern methods are also available, e.g. [4]. Modern finite element methods allow very detailed analyses of the three-dimensional state of stress in the vicinity of the end of the dropped layers, many of them are cited in [1]. All the stress based approaches have the disadvantage that all the details about the bonding layers between the dropped layer and the surrounding laminate have to be known. In real structures, neither the thickness of the bonding layers nor the shear modulus and the maximum allowed shear stress are known. Moreover, fracture criteria have to be applied to get a prediction of the strength of the laminate. There are a lot of different criteria cited in [1] starting from maximum stress criteria, the Tsai-Wu and modified Tsai-Wu criteria to very sophisticated delamination criteria. All this makes the stress approach difficult to apply for an engineer in design and analysis departments.

Methods based on the strain energy release rate do not depend so much on single material properties but more on general energy expressions. Investigations about the use of the strain energy release rate with respect to delamination analyses started in the early 90s. In [5] the strain energy release rate in tapered laminates under tension loads is investigated, in [7] and [9] the basic theory for the analytical determination of the strain energy release rate as well as experimental results are presented.

The intention of this paper is to clarify the assumptions and theories on which the resulting equations are based and to show the applicability of both approaches for the analysis of delaminations as well as bonded joints. Therefore, not only the resulting equations are given but also the background which is necessary to understand them.

2. TAPERED LAMINATE AS BONDED JOINT

In bonded joints the adhesive layer is mainly loaded by shear stresses due to different strains in both adherends. The maximum peak shear stress always occurs at the end of the stiffer adherend. Experiments show that for stiff adhesives as they are used in aerospace applications, the fracture is caused by this maximum peak shear stress [8], [9]. According to local equilibrium, the change in shear stress along the bonded layer is directly related to transverse stresses in the adhesive layer. These transverse tension stresses are known as peeling stresses. It can be shown that the peeling stresses barely influence the magnitude of the peak shear stress. For this reason, peeling stresses are often neglected in first estimations. However,

it must be noted that the peeling stresses may play an important role in the delamination process especially when the additional layers are added on the outer side of the laminate.

In the following, we assume that the bending stiffness of the adherends shall be zero. Thus, the peeling stresses are neglected, and only the shear stresses in the adhesive layer are considered. For the simple step shear lap-joint, the resulting shear stress distribution along the adhesive layer can be calculated by the classical shear-lag theory. This theory can be applied to shear loaded structures like tapered tubes as well.

2.1. Bonded laminate under tension loading

A simple step lap-joint under tension loading is considered. An additional layer with the tension stiffness E_1t_1 is bonded to the continuous laminate with the stiffness E_2t_2 (Fig. 2, t: layer thickness). The adhesive layer transfers the load by shear stresses τ_k only, the Young's modulus of the adhesive is neglected.

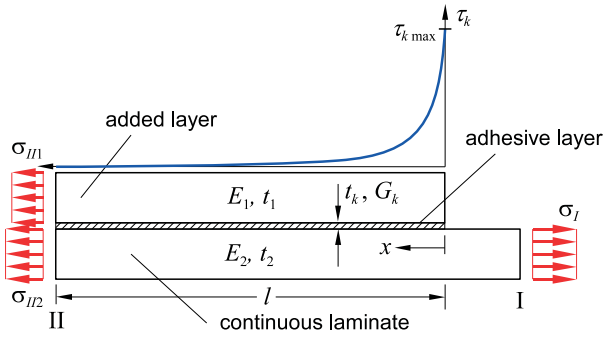

Fig. 2. Step lap-joint under tension loading; geometry and shear stress distribution in the adhesive layer

The derivation of the governing differential equation (1) for the shear stress τ_k in the adhesive layer between both laminates is given in textbooks (e.g. [10]). G_k and t_k denote the shear modulus and the thickness of the adhesive layer, respectively.

$$(1) \qquad \frac{\partial^2 \tau_k}{\partial x^2} - \tau_k \frac{G_k}{t_k}\left(\frac{1}{E_1 t_1} + \frac{1}{E_2 t_2}\right) = 0 \,.$$

Let the laminate be loaded at location I by the normal stress σ_I in the continuous laminate. Further it is assumed that at location II the ends of the laminate and of the added layer are fixed together, so that there is no difference displacement at this point and thus the shear stress is zero. With these boundary conditions, the analytical solution of (1) is given by

$$(2) \qquad \tau_k = \frac{1}{\alpha}\frac{G_k}{t_k}\frac{\sigma_I}{E_2}\frac{\sinh(\alpha l - \alpha x)}{\cosh(\alpha l)}$$

$$\text{with } \alpha = \sqrt{\frac{G_k}{t_k}\left(\frac{1}{E_1 t_1} + \frac{1}{E_2 t_2}\right)} \,.$$

The maximum shear stress τ_{kmax} occurs at $x = 0$. For a large overlapping length l the quotient of the hyberbolic functions in (2) result in 1 and thus the maximum shear stress becomes independent of the length l:

$$(3) \qquad \tau_{k\,max} = \frac{\sigma_I}{E_2}\sqrt{\frac{G_k}{t_k}}\sqrt{\frac{E_1 t_1 E_2 t_2}{E_1 t_1 + E_2 t_2}} \,.$$

With the strain $\varepsilon_I = \sigma_I / E_2$ this equation becomes:

$$(4) \qquad \tau_{k\,max} = \varepsilon_I \sqrt{\frac{G_k}{t_k}}\sqrt{\frac{E_1 t_1 E_2 t_2}{E_1 t_1 + E_2 t_2}} \,.$$

If the ultimate shear strength τ_{kmax} of the adhesive is known, the strain in the continuous layer ε_I, at which delamination occurs, can be determined from this equation:

$$(5) \qquad \varepsilon_I = \tau_{k\,max} \sqrt{\frac{t_k}{G_k}}\sqrt{\frac{E_1 t_1 + E_2 t_2}{E_1 t_1 E_2 t_2}} \,.$$

2.2. Bonded laminate under shear loading

For a laminate loaded in shear according to Fig. 3, the same equations can be applied with the only difference that the tension stiffnesses Et of the adherends have to be substituted by the corresponding shear stiffnesses Gt. Such shear loadings for instance occur at bonded tubes or at load introduction areas of shear panels.

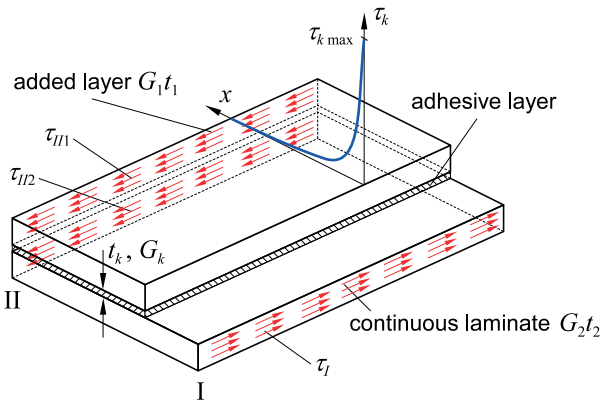

Fig. 3. Step lap-joint under shear loading, geometry and shear stress distribution in the adhesive layer

The differential equation for this case reads

$$(6) \qquad \frac{\partial^2 \tau_k}{\partial x^2} - \tau_k \frac{G_k}{t_k}\left(\frac{1}{G_1 t_1} + \frac{1}{G_2 t_2}\right) = 0 \,.$$

Let the laminate be loaded by a shear stress τ_I at location I, and let both ends of the adherends at location II be fixed together. In analogy to (3) and (4) the maximum shear stress and shear strain in the adhesive layer are given by

$$(7) \qquad \tau_{k\,max} = \frac{\tau_I}{G_2}\sqrt{\frac{G_k}{t_k}}\sqrt{\frac{G_1 t_1 G_2 t_2}{G_1 t_1 + G_2 t_2}} \,,$$

$$(8) \qquad \tau_{k\,max} = \gamma_I \sqrt{\frac{G_k}{t_k}}\sqrt{\frac{G_1 t_1 G_2 t_2}{G_1 t_1 + G_2 t_2}} \,.$$

From equation (8), the shear deformation γ_I, which results in delamination can be determined:

$$(9) \qquad \gamma_I = \tau_{k\,max} \sqrt{\frac{t_k}{G_k}}\sqrt{\frac{G_1 t_1 + G_2 t_2}{G_1 t_1 G_2 t_2}} \,.$$

2.3. Application of shear-lag theory

In practical applications, the use of the results of the shear-lag theory is difficult because there are three unkown parameters in equations (5) and (9). In both equations, the delamination strain and shear deformation depend on the parameter

(10) $\tau_{k\max}\sqrt{t_k / G_k}$.

For a given tapered laminate, the thickness t_k of the adhesive layer and the shear modulus G_k of the adhesive as well as the ultimate peak shear strength $\tau_{k\max}$ are often unknown.

Normally additional layers are added to the laminate in the non-cured state. This means that there is no special adhesive applied between the continuous laminate and the added layers. Therefore there is no discrete bonding layer and no thickness can be given.

Another difficulty results from the need for fracture criteria, when using the stress information of the shear-lag theory. There are many different criteria [1], most of them require a full three-dimensional state of stress, and a lot of strength parameters which are not available too.

Therefore the stress analysis done by the classical shear-lag theory is very helpful to get an overview about the loading mechanism of stepped bonded joints, but it is not really useful for designing tapered laminates.

In principle, it is possible to overcome these problems by not measuring the single parameters t_k, G_k and $\tau_{k\max}$ but by measuring the whole expression (10). However, the disadvantage of this procedure is that (10) is an abstract quantity that does not have a physical meaning.

3. TAPERED LAMINATE AS FRACTURE MECHANICS PROBLEM

Another way to consider the delamination problem is to use energy expressions which are more global quantities. In fracture mechanics the so-called strain energy release rate G plays an important role. The critical strain energy release rate G_c describes the strain energy which will be released when the crack becomes unstable.

In the context of delaminations inside a laminate, the fracture modes II and III are of special interest (Fig. 4). Fracture Mode II describes the delamination due to in-plane normal forces while fracture mode III describes delamination due to shear forces.

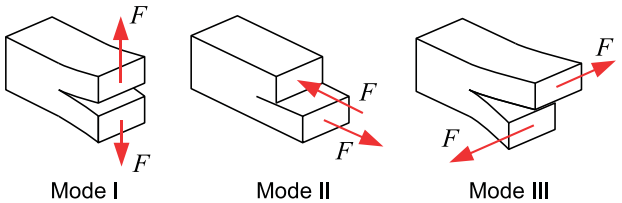

Fig. 4. Fracture modes I to III

Combined mode I/II modes occur when the additional layers are bonded on top of a laminate. In these cases in addition to the shear stresses in the adhesive layers the peeling stresses are also important and have to be considered.

3.1. Bonded laminate under tension loading (Mode II)

For the given task of an added layer, the strain energy release rate can be derived easily. Assume a crack of the length a in the adhesive layer between the added layer and the base laminate (Fig. 5). Let the crack propagate a little further by the length δa. Then the strain energy release rate is defined as the difference of the strain energy between both states related to the increase of the fracture surface.

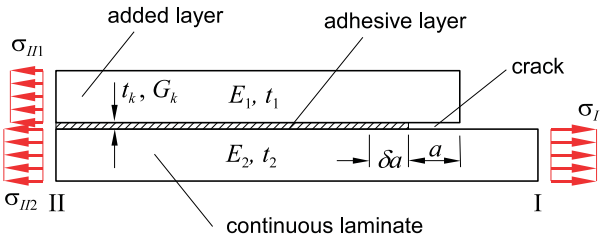

Fig. 5. Step lap-joint with crack in adhesive layer

The strain energy in the non cracked section of the laminate with length δa is given by

(11) $\Pi_{II} = \frac{1}{2}\int \sigma\varepsilon dV = \frac{1}{2}\left(\sigma_{II1}\varepsilon_{II1}t_1 + \sigma_{II2}\varepsilon_{II2}t_2\right) b\delta a$.

Substituting σ by ε and taking into account the compatibility between laminate und added layer at location II ($\varepsilon_{II1} = \varepsilon_{II2} = \varepsilon_{II}$) result in

(12) $\Pi_{II} = \frac{1}{2}\varepsilon_{II}^2\left(E_1t_1 + E_2t_2\right) b\delta a$.

The strain energy in the cracked state can be written as

(13) $\Pi_I = \frac{1}{2}\int \sigma\varepsilon dV = \frac{1}{2}\sigma_I\varepsilon_I bt_2\delta a$ or $\Pi_I = \frac{1}{2}\varepsilon_I^2 E_2t_2 b\delta a$.

The strain energy release rate G_c is defined as

(14) $G_c = \frac{\Pi_I - \Pi_{II}}{b\delta a} = \frac{1}{2}\left[\varepsilon_I^2 E_2t_2 - \varepsilon_{II}^2\left(E_1t_1 + E_2t_2\right)\right]$.

With the relation between the strain ε_I in front of the crack (location I) and ε_{II} behind the crack (location II)

(15) $\varepsilon_I = \varepsilon_{II}\frac{E_1t_1 + E_2t_2}{E_2t_2}$

the critical strain energy release rate G_c becomes

(16) $G_c = \frac{\varepsilon_{II}^2}{2}\frac{E_1t_1}{E_2t_2}\left(E_1t_1 + E_2t_2\right)$.

Inspite of the simplifications, this value is in very good agreement to 3D-finite element analyses [11].

If the strain energy release rate for a given material is known, the delamination strain ε_I can be calculated from this equation by:

(17) $\varepsilon_I = \sqrt{2G_c\frac{E_1t_1 + E_2t_2}{E_1t_1E_2t_2}}$.

The corresponding normal stress in the continuous laminate at location I follows from

$$(18)\quad \sigma_I = E_2\sqrt{2G_c\frac{E_1t_1+E_2t_2}{E_1t_1E_2t_2}}\,.$$

At location II, due to the different stiffnesses of the adherends, the normal stresses σ_{II} are

$$(19)\quad \sigma_{II2} = E_2\sqrt{2G_c\frac{E_2t_2}{E_1t_1\left(E_1t_1+E_2t_2\right)}}$$

and

$$(20)\quad \sigma_{II1} = E_1\sqrt{2G_c\frac{E_2t_2}{E_1t_1\left(E_1t_1+E_2t_2\right)}}$$

in the continuous laminate and the added layer, respectively.

3.2. Bonded laminate under shear loading (Mode III)

For an added layer under shear loading, similar equations can be derived. With the strain energies under pure shear

$$(21)\quad \Pi_{II} = \frac{1}{2}\gamma_{II}^2\left(G_1t_1+G_2t_2\right)b\delta a \quad \text{and}$$

$$(22)\quad \Pi_I = \frac{1}{2}\gamma_I^2G_2t_2b\delta a\,,$$

the critical strain energy release rate G_c becomes

$$(23)\quad G_c = \frac{1}{2}\left[\gamma_I^2G_2t_2-\gamma_{II}^2\left(G_1t_1+G_2t_2\right)\right].$$

With the relation between the shear strains γ_I and γ_{II}, G_c can be written as

$$(24)\quad G_c = \frac{\gamma_{II}^2}{2}\frac{G_1t_1}{G_2t_2}\left(G_1t_1+G_2t_2\right).$$

If the strain energy release rate for a given material is known, the delamination strain γ_I and shear stress τ_I at location I can be calculated:

$$(25)\quad \gamma_I = \sqrt{2G_c\frac{G_1t_1+G_2t_2}{G_1t_1G_2t_2}}\,,\quad \tau_I = G_2\sqrt{2G_c\frac{G_1t_1+G_2t_2}{G_1t_1G_2t_2}}\,.$$

The shear stresses at location II can be written analogous to equations (19) and (20).

4. COMPARISON BETWEEN SHEAR-LAG THEORY AND STRAIN ENERGY RELEASE RATE

In Tab. 1 the results of the shear-lag theory and the energy based procedure are compared. It is obvious that both theories yield very similar equations, especially the stiffness related terms are the same. The only differences are the way, the properties of the adhesive layer are considered. As shown in (10), the stress based procedure requires three different properties of the adhesive layer while the energy based procedure gets by with only one parameter.

Equalizing the corresponding equations yield a relation between the critical strain energy release rate G_c and the properties of the adhesive layer t_k, G_k and $\tau_{k\max}$ (26). Thus, the three unknown stress properties can be substituted by only one parameter, which can be easily determined by tests. It must be noted that this equation is the same for both fracture modes, mode II and mode III.

$$(26)\quad G_c = \frac{1}{2}\tau_{k\max}^2\frac{t_k}{G_k}\,.$$

The right side of (26) can be considered as strain energy Π_k of the adhesive layer with an infinitesimal length δa, which will be released when the crack propagates related to the crack surface $b\delta a$:

$$(27)\quad \Pi_k = \frac{1}{2b\delta a}\int\tau_{k\max}\gamma_k dV = \frac{1}{2}\tau_{k\max}^2\frac{t_k}{G_k} = G_c\,.$$

TAB 1. Comparison of delamination strain determined by different theories

Delamination strain ε_I, γ_I, (shear-lag theory)	Delamination strain ε_I, γ_I, (energy approach)
$\varepsilon_I = \tau_{k\max}\sqrt{\frac{t_k}{G_k}}\sqrt{\frac{E_1t_1+E_2t_2}{E_1t_1E_2t_2}}$	$\varepsilon_I = \sqrt{2G_c\frac{E_1t_1+E_2t_2}{E_1t_1E_2t_2}}$
$\gamma_I = \tau_{k\max}\sqrt{\frac{t_k}{G_k}}\sqrt{\frac{G_1t_1+G_2t_2}{G_1t_1G_2t_2}}$	$\gamma_I = \sqrt{2G_c\frac{G_1t_1+G_2t_2}{G_1t_1G_2t_2}}$

5. EXPERIMENTAL RESULTS RELATED TO THE ROTOR BLADES OF THE HELICOPTERS EC 135 AND EC 145 OF EUROCOPTER

The “Bearingless Main Rotor” is one of the most outstanding features of the helicopter EC 135. Whereas the rotor hub is a very simple metal design, the blade structure has become complicated (Fig. 6). Many features such as the hinges were introduced into the blade design. The blade’s local stiffnesses and cross sections had to be adapted to the local needs of the structure.

The stiff rotor blade attachment is fastened to the rotor hub by two bolts. In the transition zone between attachment and “flapping hinge” the glass fibre unidirectional E-Glass/913 laminate had to be tapered. Furthermore the laminates had to be shifted to a cruciform cross section for the torsion loaded structural element. The two areas of ”flapping hinge” and “cruciform torsion cross section” could be designed independently, only connected by tapered transition elements [12].

The blade is loaded by static and dynamic centrifugal force, bending and torsional moments. Thus the transition zone between attachment and the “flapping hinge” is mainly loaded by the centrifugal load and flapping bending moments, whereas the transition zone between “flapping hinge” and cruciform torsional element is loaded by centrifugal forces and torsional moments.

Fig. 6. 3-Dimensional structure of the EC 135 “Flex-beam” attachment, “flapping hinge” and cruciform torsional structural element (from right to left)

The certification procedure included the testing of coupons and structures. Static and dynamic structural testing revealed the critical areas of the design. The helicopter was certified according to the European Joint Aviation Requirements JAR 27. For the design of the rotor blade, the LBA (Luftfahrtbundesamt) established special conditions for primary structures designed with composite materials. One special demand consisted in the establishment of the residual strength after applying dynamic loads to the structure. On the basis of the certification requirements, the delamination behaviour, especially of the transition zones of the blade, had to be investigated in detail.

Delaminations were studied with the help of fracture mechanics coupons, mainly considering mode II and III. The influence of mode I was accounted for in the design of the structure by avoiding mode I stresses. For the evaluation of consequences of mode II effects, the critical energy release rate was determined.

Strain energy release rates can be measured very effectively by the use of so called TCT (Transverse Crack Tension) specimens (Fig. 7), [12]. The specimen is loaded in tension and at a certain tension force, a crack develops at the ends of the cut layers. From this fracture load, the strain energy release rate can be calculated by equation (18), (19) or (20).

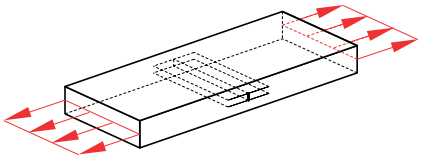

Fig. 7. The Transverse Crack Tension Specimen (TCT) for measuring the strain energy release rate G_c

As an example, Table 2 shows the measured fracture stress σ_{II2} and Young’s Modulus E for different materials ($E_1 t_1 = E_2 t_2 = Et$). By the use of equation (19), the critical strain energy release rate is determined from this data. The strain energy release rate is influenced by the stiffness of the fibre-composite. Even though the strain energy release rate for materials with higher stiffness decreases, the delamination strength σ_{II2} remains at least constant.

TAB 2. Delamination strength σ_{II2}, Young´s modulus E and critical strain energy release rate G_c according to (19) for different prepregs

	σ_{II2} N/mm^2	E N/mm^2	G_c N/mm
E-Glass / 913	779	43060	1,101
R-Glass / 913	897	47790	1,315
T300 / 913	1141	135700	0,750

In Figure 8 S-N curves for the critical delamination upper strength related to E-Glas/913, R-Glas/913 and T300/913 are given. The S-N curve for carbon-composite T300/913 shows high strength values for low and especially for high cycle fatigue.

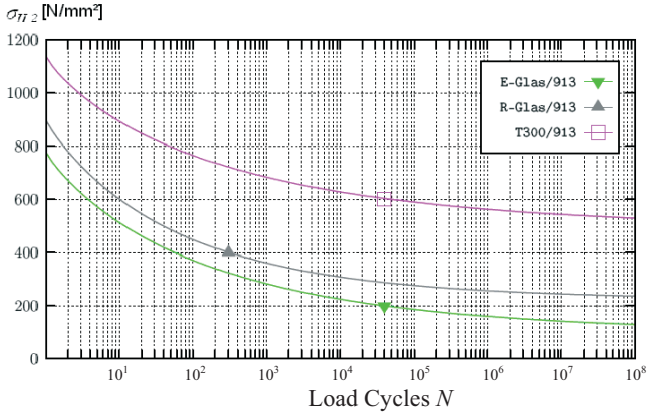

Fig. 8. The critical delamination strength, considered in the S-N-curve as upper strength with the stress-ratio of R = 0, versus load cycles N

The multi-mission transport helicopter EC 145 was derived from the BK 117 with a modified rotor (Fig. 9). The blade consists of a basic fibre-composite structure attached to a titanium fitting. A metallic erosion strip is bonded to the blade body as shown in Figure 10.

Fig. 9. The EC 145 multi-mission transport helicopter of Eurocopter

For the certification of the rotor, coupon tests under static and dynamic loading were performed. For different combinations of adherends such as steel/glass-composite, titanium/glass-composite and aluminum/aluminum the specimens were defined. In Figure 11 the specimen for the

combination of the adherends steel/glass-composite bonded together with the adhesive FM 73 is shown. The glass-composite is an unidirectional lay up.

Fig. 10. The rotor blade of the EC 145 with load introduction fitting and metallic erosion strip, bonded to the composite blade structure

The specimens were loaded in tension, the peek shear-stresses were calculated from equation (3). With the measured thickness of the adhesive FM 73 and the shear modulus of 680 N/mm² the strain energy release rate of the bonded joint could be determined by equation (26). In Table 3 the measured adhesive thicknesses for the different adherends, the peak shear strengths and the strain energy release rates under static and dynamic loads are given. The stresses in the adhesive and in the adherends are estimated to be in the elastic range.

TAB 3. Double lap shear test results with titanium, steel and aluminum plates bonded to glass-fibre-composites (GFRP). The strain energy release rate G_c is calculated from equation (26)

Material Comb.	t_k mm	τ_{kmax} N/mm^2	G_c static N/mm	$\tau_{kmax,\,dyn}$ 10^7 cyc. N/mm^2	$G_{c,\,dyn}$ 10^7 cyc. N/mm
Ti/GFRP	0,20	52,9	0,40	24,8	0,09
St/GFRP	0,13	67,3	0,42	37,9	0,14
Al/Al	0,19	48,3	0,33	25,7	0,09

The S-N-curves for the upper shear strength with a stress ratio of R=0 for the different adherends, bonded together with the adhesive FM 73, are shown in the Figures 12, 13 and 14. Figure 12 shows the test results for titanium plates bonded to glass-fibre-composites. Two batches of specimens (testplate 1 and 2) were tested. For the steel plate bonded joints, shown in Figure 13, higher values are achieved in the low cycle domain. The high cycle fatigue strength values for steel joints are much higher than the values for the titanium joints. For the aluminum/aluminum bonded joints (Figure 14) the low cycle fatigue strengths are quite low, but the high cycle fatigue strength is in the range of the titanium/glass-fibre-composite joint.

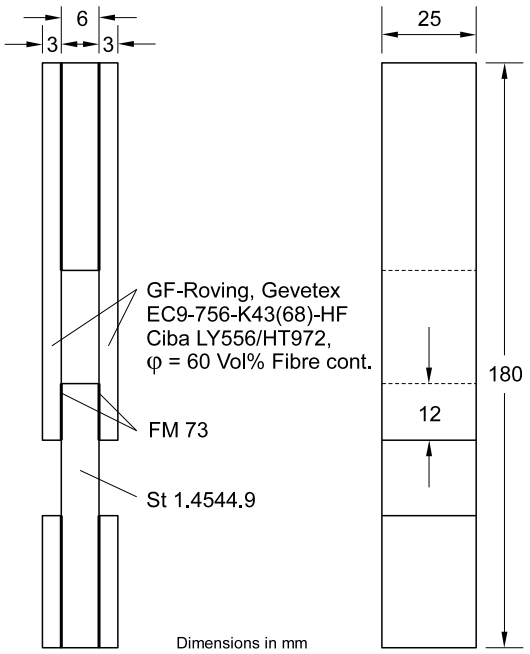

Fig. 11. Double lap shear specimen with E-Glas-fibre-composites bonded to steel plates

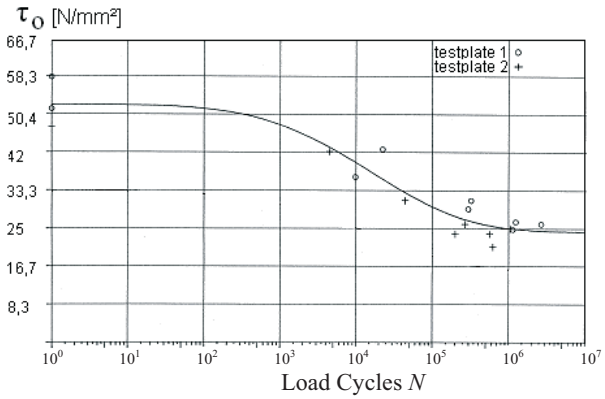

Fig. 12. S-N-curve for the upper shear strength values of titanium plates bonded to glass-fibre-composite by FM 73

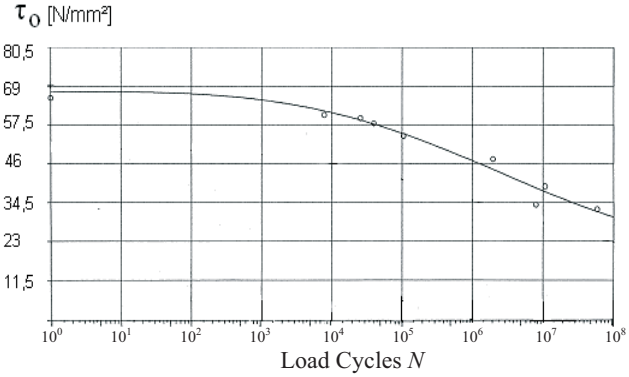

Fig. 13. S-N-curve for the upper shear strength values of steel plates bonded to glass-fibre-composite by FM 73

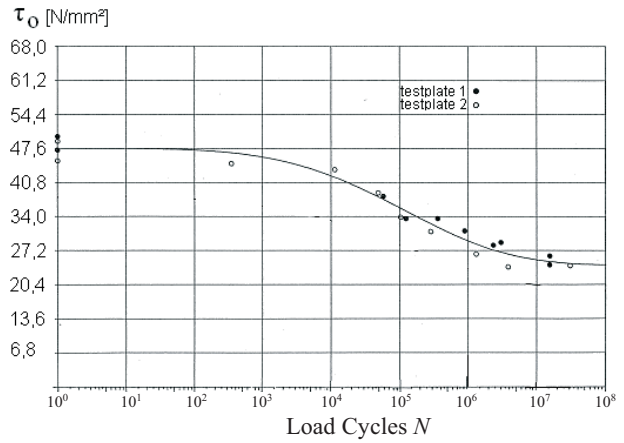

Fig. 14. S-N-curve for the upper shear strength values of aluminum plates bonded to aluminum plates by FM 73

6. SUMMARY AND FUTURE DEVELOPMENTS

In current developments, especially regarding helicopter structures, fibre composites are of outstanding importance. These structures have to withstand environmental conditions, static and dynamic loads. Due to weight reasons the components made from fibre reinforced materials have to be designed with variable cross section geometry, layers have to be added or dropped to or from laminates.

The rotor blade of a helicopter needs an erosion strip to protect the blade body from damage, it has to be bonded to the fibre reinforced structure. Huge areas of carbon-fibre-composite laminates are joined together for big aircraft fuselages. In case of damage, composite patches have to be bonded to the basic structure.

All these structures are sensitive to delaminations which have to be analysed thoroughly. Finite element methods and the shear-lag theory are standard tools for the characterisation of joints. A fracture mechanics approach by the use of the strain energy release rate opens new possibilities to analyse bonded step-lap joints, tapered laminates and butt joints. This energy based approach has the advantage that only one strength parameter, the strain energy release rate, has to be determined whereas the application of the stress based shear lag theory requires three parameters as well as fracture criteria. Therefore the energy approach may significantly simplify the analysis of these design tasks.

The interaction between the application of fracture mechanics and the shear-lag theory to different joints is shown. The critical strain energy release rate is a characteristic material value which can be measured by test and can be used for the design of bonded and tapered structures. Results of tests are presented. New application areas of this approach are the design of impacted areas and the characterisation of improved composites.

7. REFERENCES

[1] He, K., Hoa, S. V., Ganesan, R., The study of tapered laminated composite structures: a review. Composite Science and Technology, 60 (2000), 2643 – 2657

[2] Volkersen, O., Die Schubkraftverteilung in Leim-, Niet- und Bolzenverbindungen. Energie und Technik 5 (1953), H. 3, 5 and 7

[3] Goland, M. and Reissner, The stresses in cemented joints. E. J. Appl. Mech., 11 (1944), A17 – A27

[4] Vizzini A. J., Shear-Lag Analysis about an Internally-Dropped Ply. Journal of Reinforced Plastics and Composites, 16 (1997) 1, 73 – 85

[5] Salpekar, S. I., Raju I.S., O'Brian, T.K., Strain-energy-release rate analysis of delamination in a tapered laminate subjected to tension load. Journal of Composite Materials, 25 (1991), 118 – 141

[6] Wisnom, M. R., Prediction of Delamination in Tapered Unidirectional Glass Fibre Epoxy with Dropped Plies under Static Tensions and Compressions. AGARD-SMP Specialist´s Meeting on Debonding/Delamination of Composites, 25-27 May. 1992

[7] Wisnom, M. R., On the Increase in Fracture Energy with Thickness in Delamination of Unidirectional Glass Fibre-Epoxy with Cut Central Plies, Journal of Reinforced Plastics and Composites, 11 (1992) 897 – 909

[8] Bansemir, H., Festigkeit von dynamisch beanspruchten Krafteinleitungen für Faserverbundrotoren, Paper No. 87-108, DGLR-Jahrestagung, Berlin, 1987

[9] Wolfrum, J., Schade, M., Rapp H., Vorhersage der Festigkeit geschäfteter Klebeverbindungen, adhäsion, 9 (2007), 46 – 48

[10] Schürmann, H., Konstruieren mit Faser-Kunstsoff-Verbunden, Springer Verlag Berlin, 2005

[11] Weicheng, C., Wisnom, M. R., Jones, M., An Experimental and Analytical Study of Delamination of Unidirectional Specimens with Cut Central Plies, Journal of Reinforced Plastics and Composites, 13 (1994) 722 - 739

[12] Bansemir, H., Emmerling, S., Fatigue Substantiation and Damage Tolerance Evaluation of Fibre Composite Helicopter Components, Applied Vehicle Technology Panel: Applications of Damage Tolerance Principles for Improved Airworthiness of Rotorcraft, Corfu, Greece, April 21 – 22, 1999

[13] Bansemir, H., Burghagen, S., Gädke, M., Das Delaminationsverhalten von Unidirektionalverbunden als Grundlage für die Charakterisierung und Dimensionierung von FVW-Strukturen, DGLR-Kongress 2005, Friedrichshafen, 25.-29. September

[14] Weiß, W., Wöhlerlinien von Zugscherproben unter Zugschwellbelastung, Eurocopter Deutschland, TN-DE133-7/82, 21.04.1982